NAVAL SURFACE WEAPONS CENTER
WHITE OAK, SILVER SPRING, MARYLAND 20910

HEAT TRANSFER MEASUREMENTS DURING RAPID PITCH SWEEPS USING COAXIAL THERMOCOUPLES

BY

J. A. F. HILL
W. C. RAGSDALE
E. R. HEDLUND
R. L. P. VOISINET

PRESENTED AT THE

54th SEMI-ANNUAL MEETING

OF THE

SUPERSONIC TUNNEL ASSOCIATION

SPONSORED BY

GRUMMAN AEROSPACE

NEW YORK UNIVERSITY AND

POLYTECHNIC INSTITUTE OF

NEW YORK

NEW YORK CITY, NEW YORK

9-10 OCTOBER, 1980

I. INTRODUCTION

This paper describes the introduction of the coaxial thermocouple technique to the Hypervelocity Tunnel (Tunnel 9) at the Naval Surface Weapons Center (NSWC) White Oak Laboratory. It describes our experience during both a short shakedown test and the first production test in which the heat transfer was measured at 113 locations on a model of the space shuttle orbiter.

To utilize the coaxial thermocouple technique the model wall is made thick enough that it may be considered a semi-infinite slab as far as transient heat conduction is concerned. The coaxial thermocouple is inserted through the wall so that the outer surface temperature may be measured using wires emerging from the back surface (see Figure 2). Extensive previous use of the coaxial thermocouple technique at AEDC had demonstrated the following desirable features;

-it is rugged

-it requires no calibration

-it may be contoured exactly to the model surface

-it has a very short response time

-it may be made very small, allowing very close spacing of adjacent thermocouples

Before adopting it for routine use in Tunnel 9 we had to consider the following questions;

Can the model wall conveniently be made thick enough to be considered semi-infinite?

Can the available data reduction techniques (for our given sampling rates) handle the variations in heat transfer associated with our rapid pitch sweeps?

Preliminary calculations showed the answers to be favorable. The next step was a shakedown test to actually demonstrate feasibility.

This test was successful and the technique has since been used for measurements of the heat transfer rates on a model of the space shuttle orbiter.

II. WIND TUNNEL

Both test programs discussed in this paper were conducted in the Hypervelocity Tunnel at the White Oak Laboratory of the Naval Surface Weapons Center. At Mach 14 the Reynolds number in the first test was 3.7×10^6 per foot while in the second test values of 3.6×10^6 and 1.8×10^6 per foot were used. The time history of the nozzle supply conditions in this tunnel is shown in Figure 1. Note that it takes about 0.6 seconds for the supply conditions to stabilize and the flow to become free of condensation. The useable data is obtained during the next 0.7 seconds. The total time during which the model is subjected to heating is about 1.3 seconds.

III. THERMAL CHARACTERISTICS OF THE THERMOCOUPLE MATERIALS AND MODEL WALL

The construction of a coaxial thermocouple is shown schematically in Figure 2. A chromel wire is surrounded by electrical insulation and an outer constantan jacket. This assembly is inserted in the model wall so that the tip of the thermocouple is flush with the model wall. The tip may be sanded to conform to the model contour and the thermocouple junction is made as the two metals are blended together by the action of the sandpaper.

The material property which governs the temperature response of a semi-infinite slab to surface heating is the product ρck where

ρ is the density

c is the specific heat

k is the thermal conductivity

For the coaxial thermocouple scheme to work the value of this lumped thermal parameter should be the same for both thermocouple materials and the model wall material, since in that case the wall may be treated mathematically as homogenous. The following table shows that this condition is quite well satisfied if the model is constructed of 17-4 PH stainless steel.

	$(\rho ck)^{\frac{1}{2}}$, Btu/ft^2-sec$^{\frac{1}{2}}$-^{o}F
chromel	.410
constantan	.408
17-4 PH stainless steel	.409

The other condition which must be satisfied for the data reduction scheme to be valid is that the temperature rise at the front surface not be affected by the boundary condition at the back surface. To express this condition in terms of the model wall parameters we have used the solution given in reference 1 for the one dimensional flow of heat into a perfectly insulated slab with constant heat flux at the front surface. The temperature thus obtained has been substituted into the constant-heat flux solution for the semi-infinite slab

$$\dot{q}_o = \frac{\sqrt{\pi \rho c k}}{2} \frac{T_w}{\sqrt{t}} \qquad (1)$$

and the difference between this result and the originally given constant heat flux $\dot{q}_o$ has been computed. Figure 3 shows this error in terms of the parameter $L/\sqrt{\alpha t}$

L is the wall thickness

α is the thermal diffusivity $k/\rho c$

The figure shows that the error is

negligible for $L/\sqrt{\alpha t} > 2.2$

less than 1% for $L/\sqrt{\alpha t} > 1.8$

Now the values of $\sqrt{\alpha}$ for the three materials are

	$\sqrt{\alpha}$ (in. $\sec^{-\frac{1}{2}}$)
Chromel	.085
Constantan	.094
17-4 PH stainless steel	.084

Using the mean of these values the wall thickness required to limit the error to 1% after 1.3 seconds is

$$L_{min} = 0.18 \text{ inches} \qquad (2)$$

IV. DATA ACQUISITION AND REDUCTION

The voltage signals from the coaxial thermocouples were amplified, digitized and recorded on the DARE V data acquisition system of the Hypervelocity Tunnel.

The sampling rate was 250/sec in the first test and 100/sec in the second test.

For the data reduction we used standard methods given in the literature and previously investigated at AEDC and elsewhere.

The heating rate at each thermocouple location was computed from the surface temperature history measured by the coaxial thermocouple, based on the assumption that the model behaved as a semi-infinite slab with heat conduction perpendicular to the surface. In this case the relationship between the surface temperature and the heating rate is given by the theory of one-dimensional heat conduction into a homogenous semi-infinite solid (Ref. 1,2), as follows:

$$\dot{q}(t) = \left(\frac{\rho c k}{\pi}\right)^{1/2} \int_0^t \frac{dT(\tau)}{d\tau} \frac{d\tau}{(t-\tau)^{1/2}} \qquad (3)$$

where $q(t)$ = heating rate at surface, Btu/ft.^{2}-sec.

t = time, from start of heating, sec.

$T(t)$ = surface temperature rise, ^oF

τ = dummy variable of integation

The cumulative heat input from the start of heating up to time t is given by a similar equation:

$$Q(t) = \left(\frac{\rho c k}{\pi}\right)^{\frac{1}{2}} \int_0^t \frac{T(\tau)}{(t-\tau)^{\frac{1}{2}}} \, d\tau \qquad (4)$$

where $Q(\tau)$ = cumulative heating, Btu/ft^2

and finally,

$$q(t) = \frac{dQ(t)}{dt} \qquad (5)$$

Implicit in equations (1) and (2) is the assumption that the temperature is uniform within the semi-infinite solid at the start of heating.

The first method may be called a direct method, in that $\dot{q}(t)$ is obtained directly. To use it is generally necessary to eliminate any noise from the data before integration. The second method is indirect, in that $Q(t)$ is obtained first and then differentiated to obtain $\dot{q}(t)$. Here the integration tends to smooth the data and no preliminary noise reduction is necessary.

Practical finite-difference methods for carrying out the computations in equations (3) and (4) have been given in the literature. For the direct method Cook and Felderman (ref. 3) give

$$\dot{q}(t_n) = \left(\frac{\rho c k}{\pi}\right)^{1/2}\left[\frac{T(t_n)}{\sqrt{t_n}} + \sum_{i=1}^{n-1}\left\{\frac{T(t_n)-T(t_i)}{(t_n-t_i)^{1/2}} - \frac{T(t_n)-T(t_{i-1})}{(t_n-t_{i-1})^{1/2}} + 2\frac{T(t_i)-T(t_{i-1})}{(t_n-t_i)^{1/2}+(t_n-t_{i-1})^{1/2}}\right\} + \frac{T(t_n)-T(t_{n-1})}{\sqrt{\Delta t}}\right] \quad (6)$$

Several authors, including Schultz and Jones (ref. 4) have noted that this may be further simplified by noting that when $t_o=0$, $T(t_o)=0$ so that

$$\dot{q}(t_n) = \left(\frac{\rho c k}{\pi}\right)^{1/2}\sum_{i=1}^{n}\left[\frac{T(t_i)-T(t_{i-1})}{(t_n-t_i)^{1/2}+(t_n-t_{i-1})^{1/2}}\right] \quad (7)$$

For the indirect method (Dixon ref. 5) has given the formula

$$Q(t_n) = \left(\frac{\rho c k}{\pi}\right)^{1/2}\sum_{i=0}^{n-1}\left[\frac{T(t_i)+T(t_{i+1})}{(t_n-t_i)^{1/2}+(t_n-t_{i+1})^{1/2}}\right]\Delta t \quad (8)$$

The only approximations involved in these formulas are in the local linearaization of $T(\tau)$. For both test programs both methods were investigated and a choice was made between them as described below.

V. SHAKEDOWN TEST

The shakedown test was planned to demonstrate the validity of data obtained during rapid pitch sweeps. We also tested a model for which the wall was not thick enough to satisfy the criterion of equation (2) but in which plugs surrounding the thermocouples were installed so that equation (2) was satisfied locally.

5.1 Models and Instrumentation

The models used were sphere cones as shown in Figure 4. Both coaxial thermocouples and Gardon gages were installed. The data obtained with the Gardon gages is discussed in reference 6 but will be omitted from this paper. The locations of the coaxial thermocouples are shown in Figure 5.

5.2 Data Reduction

It was found that the results obtained from any one of equations (6), (7), or (8) were indistinguishable and equation (8) was finally chosen because it used less computation time. For presentation the results were reduced to Stanton numbers where

$$ST = \dot{q}\left[c_p \rho_\infty U_\infty (T_{01} - T_w)\right]^{-1}$$

where $\dot{q}$ = calculated heat transfer rate (Btu/ft.^{2}-sec.)

ρ_∞ = free stream density (lbm/ft^3)

U_∞ = free stream velocity (ft/sec)

c_p = heat capacity for nitrogen = 0.248 Btu/lbm-$^\circ$F

T_{01} = equivalent ideal gas supply temperature ($^\circ$R)

T_w = measured wall temperature ($^\circ$R)

$c_p T_{01}$ = equals the stagnation enthalpy

Theoretical calculations were also made using the tunnel conditions and the G. E. 3-D Viscous Code (ref. 7) for a few angles of attack.

5.3 Results

The four runs for which results are presented may be characterized as follows;

Run	Model Wall	Pitch Program
496	thick	upsweep 0° to 18°
497	↓	pitch-pause 10°
498	↓	downsweep 22° to 0°
499	thin	upsweep 0° to 18°

The results obtained at the five thermocouple locations are shown in Figures 6-10, in which the Stanton number is plotted versus angle of attack. An approximate scale of heating rate $\dot{q}$ is Btu/ft^{2}sec is given on the right-hand sides of the figures. The range of $\dot{q}$ covered is roughly 1-100 Btu/ft^{2}sec.

5.4 Discussion

The data obtained during a pitch sweep always agree quite closely with the static data obtained in the pitch-pause mode. The difference at $\alpha=10^{o}$ is never larger than about 10% and on the average is about 5%.

The dynamic data obtained during the upsweep and downsweep may fall on opposite sides of the static point and the difference between the two sweeps average about 8%. There are no clear trends in terms of which sweep gives the larger Stanton number or the variation of the difference with heat transfer rate. The best agreement occurs at the highest and lowest heat transfer rates.

Thin-wall data were obtained with thermocouples T4 and T5 only, since T3 failed. T4, with a ½ inch diameter plug, reads low and T5, with a ¼ inch diameter plug, reads high. The errors are not large, however, and data obtained with a ½ inch diameter plug may well be acceptable in general.

VI. SPACE SHUTTLE TEST

6.1 Objectives

This heat transfer test on the Space Shuttle Orbiter was sponsored jointly by the Air Force Flight Dynamics Laboratory (AFFDL) and the Johnson Space Center of NASA. The principal objectives were to:

- Extend the existing wind tunnel data base to higher Mach number
- Investigate the effect of yaw on aerodynamic heating
- Investigate areas of intense heating on the orbital maneuvering sub system (OMS) pods

Previous tests had shown that this last phenomenon was very localized and very sensitive to angle of attack, so that a continuous pitch sweep would almost certainly be required to define it. The range of angles of attack to be covered was specified to be from 20^{o} to 42^{o} and individual runs were planned for each of four yaw angles, 0^{o}, 1^{o}, 2^{o}, and 4^{o}.

6.2 Model and Instrumentation

A 0.0175 scale model was furnished by AFFDL and instrumented at NSWC. 113 coaxial thermocouples were installed at locations marked on the model by AFFDL. Figures 11 and 12 are photographs of the model showing some of the thermocouple locations.

These thermocouples were manufactured by the MEDTHERM corporation and had a diameter of 0.062 inches. As in the shakedown test the model was constructed of 17-4 PH stainless steel.

6.3 Data Reduction

A new look at data reduction procedures for these tests was required by the much more rapid variation of heating rate with time than in the shakedown test. For this purpose some synthetic data was generated in analytical form so that the output of the reduction process could be compared with an exact analytical solution.

Figures 13 and 14 show two examples of data obtained from thermocouples on the OMS pods, in terms of heating rate versus time. Parabolic curves have been fitted to these data as shown. From those curves exact values of surface temperature rise were calculated and used as synthetic data, sampled at 100 samples per second as in the test. The heating rates computed from these data are shown in Figures 15 and 16, where they are compared with the exact analytical curves. It is clear that for this kind of data the direct method does a better job with the peaks and valleys in the data, and accordingly it was chosen for reducing the space shuttle data.

We recall that when the direct method is used, the thermocouple signal may need to be smoothed before the computations given in equation (6) or (7) are carried out. Data from the Hypervelocity Tunnel is generally smoothed by simple low-pass filtering, using a digital 6th order Butterworth filter, as described reference 8. Figure 17 shows three examples of filtered and unfiltered data, for thermocouple signals exposed to a range of heating rates and hence exhibiting a range of signal-to-noise ratios. As the signal-to-noise ratio drops with decreasing values of $\dot{q}$ (and hence increasing amplifier gain), it takes lower cut-off frequencies for the filter to smooth the data. At the gains used for the extremely low heating rates ($\dot{q} \approx$/Btu/ft^2 sec) noise reduction becomes a critical issue.

The heat transfer data was reduced to Stanton numbers defined as

$$St = \dot{q} \left[\rho_\infty U_\infty c_p \ (0.9T_{01} - T_w) \right]^{-1} \qquad (10)$$

with the same nomenclature as in equation (9). For some data presentations the ratio St/St_o was used, where St_o is a reference Stanton number at the stagnation point of a 0.0175-foot radius (scaled 1-foot radius) sphere at the tunnel flow conditions.

6.4 Results

The scope of the test is indicated by the following run schedule

Run	Pitch Sweep	Yaw Angle	Nominal Unit Reynolds No.
577	14° to 43°	1°	3.6×10^{6} ft^{-1}
579	43° to 17°	1°	3.6×10^{6} ft^{-1}
580	43° to 15°	0°	1.8×10^{6} ft^{-1}
581*	43° to 15°	0°	1.8×10^{6} ft^{-1}
582	43° to 21°	0°	3.6×10^{6} ft^{-1}
583	44° to 21°	2°	3.6×10^{6} ft^{-1}
585	44° to 17°	4°	3.6×10^{6} ft^{-1}

* with boundary layer trip at X/L=0.1

Just a very small sample of the total results will be given here for illustration. Figure 18 shows a comparison of the upsweep and downsweep data on the bottom centerline. Figure 19 shows the effect of the boundary layer trip on the data for the bottom centerline. Data obtained on the OMS pods are shown in Figures 20 and 21. One shows the very large but narrow peak at $\alpha=24^{\circ}$ while the other, located only ½ inch away (model scale) shows only a small rise at low angles of attack.

6.5 Discussion

The peaks in the heating rate, localized both spatially and in terms of angle of attack, on the OMS pods appear to have been defined quite well using the rapid pitch sweeps in conjunction with the data reduction scheme described above. Note that the pitch rate was about 40 degrees/second so that the data was sampled about every 0.4 degrees.

We had some concern about lateral conduction since there are very large differences in heating rate over distances comparable with the thermocouple spacing (≃ ¼ inch). These differential heating rates build up temperature differences as large as $100^{\circ}F$. Some simple calculations have shown that the "heat sink" effect of adjacent unheated areas of the model introduces errors smaller than 5% if the Fourier number

$$\alpha t/R^2 \quad < 0.16$$

where α is the thermal diffusivity

t is the time during which the heating peak exists

R is the radius of the hot spot

Now the peak only lasts about 0.15 seconds so this criterion is satisfied if R>0.09 inches. This is compatible with a spot size of the order of the gage spacing and we may conclude that the effects of lateral conduction are not serious.

Estimates of all the errors from all sources in the heat transfer rates are given in reference 9, where the total uncertainty is estimated to lie in the range of 5% to 10%.

VII. CONCLUSIONS

1. For stainless steel models compatible with coaxial thermocouples, the minimum skin thickness required to validate the semi-infinite slab principle of data reduction in Tunnel 9 is 0.18 inches. This requirement can easily be satisfied for both R/V and space shuttle models.

2. Even when the heat transfer rate varies very rapidly with angle of attack, there is no problem in reducing data acquired at pitch rates up to at least 40 degrees/sec. Heating rates in the range 1 to 100 Btu/ft^2 sec were measured with an accuracy estimated as 5%-10%.

3. For the flow regime achieved in Tunnel 9, the ability to acquire heat transfer data continuously over a range of angles of attack is unique and constitutes a valuable tool for investigation of reentry aerodynamic heating.

ACKNOWLEDGEMENT

The authors are indebted to Carl T. Kidd of ARO, Inc. for furnishing several internal memoranda describing coaxial thermocouple techniques and helpfully answering a number of questions.

REFERENCES

1. Carslaw, H. S. and Jaeger, J. C. Conduction of Heat in Solids, Second Edition, Oxford, Clarendon Press, 1959.

2. Geidt, W. H. "The Determination of Transient Temperatures and Heat Transfer at a Gas-Metal Interface Applied to a 40-mm Gun Barrel" Jet Propulsion Volume 25, No. 4 April 1955.

3. Cook, W. J. and Felderman, E. J., "Reduction of Data from Thin-Film Heat-Transfer Gages: A Concise Numerical Technique, "AIAA Journal", Volume 4, Number 3, March 1966.

4. Schultz, D. L. and Jones, T. V., Heat Transfer Measurements in Short-Duration Hypersonic Facilities. AGARDO Graph No. 165, February 1963.

5. Kendall, D. N. and Dixon, W. P., "Heat Transfer Measurements in a Hot Shot Wind Tunnel, "Presented at the IEEE Aerospace Systems Conference, Seattle, Washington, 11-15 July 1966.

6. Hedlund, E. R. Heat Transfer Testing in the NSWC Hypervelocity Wind Tunnel Utilizing Coaxial Surface Thermocouples NSWC MP80-151, March 1980.

7. Hecht, A. M., Nestler, D. E., and Richbourg, D. H., Application of a Three-Dimensional Viscous Computer Code to Reentry Vehicle Design, AIAA Paper 79-0306, January 1979.

8. Hill, J. A. F., Stability and Pressure Measurements in the Naval Surface Weapons Center Hypervelocity Tunnel ICIASF 77 Record IEEE Aerospace and Electronic Systems Society, September 1977.

9. Ragsdale, W. C., Space Shuttle Heat Transfer Tests in the NSWC Hypervelocity Tunnel (WTR 1331) NSWC MP-80-423, September 1980.

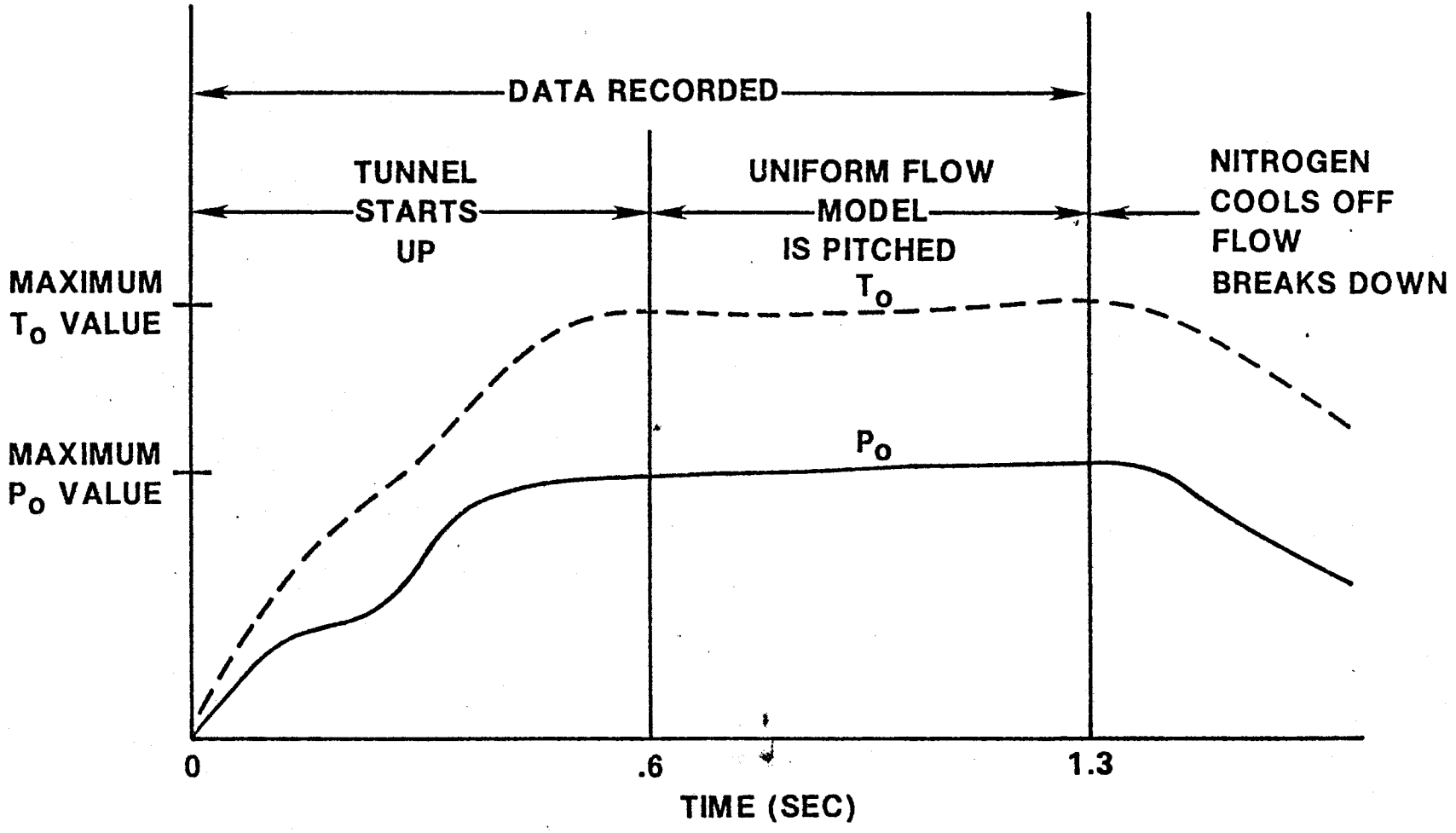

FIGURE 1 - HYPERVELOCITY TUNNEL FLOW SEQUENCE

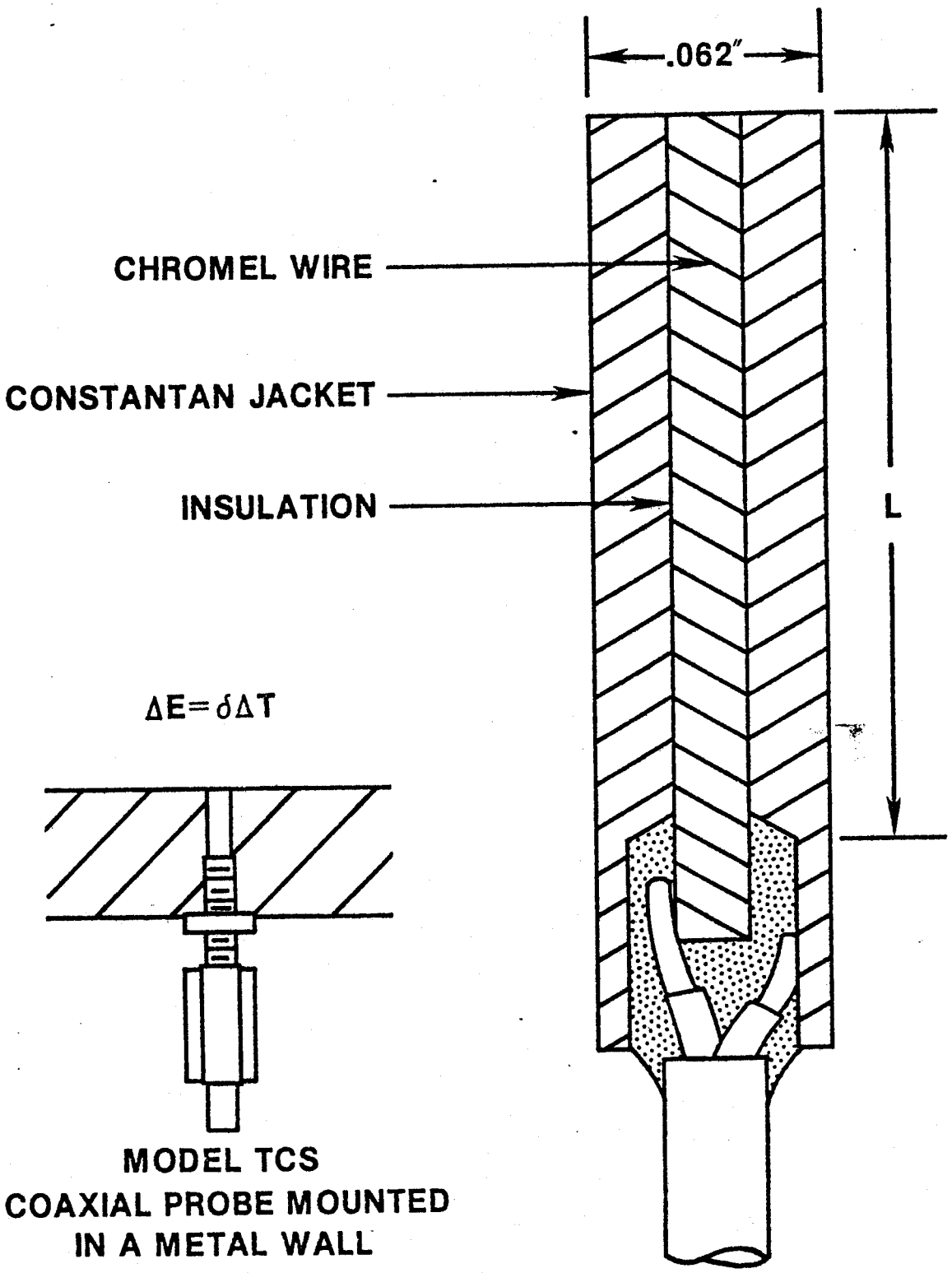

FIGURE 2 - CONSTRUCTION OF COAXIAL THERMOCOUPLE

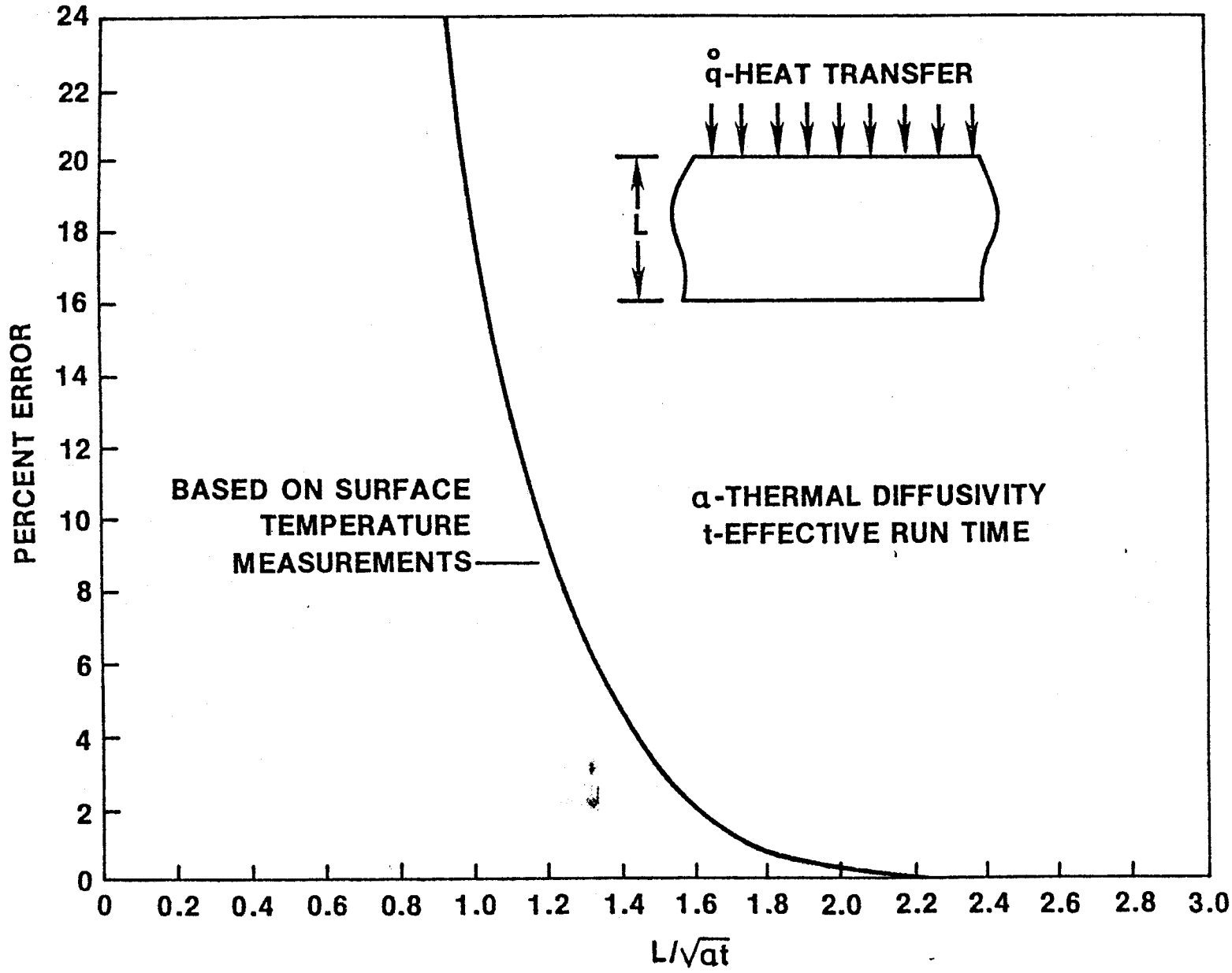

FIGURE 3 - ERROR IN HEAT TRANSFER FOR SLABS WITH FINITE THICKNESS

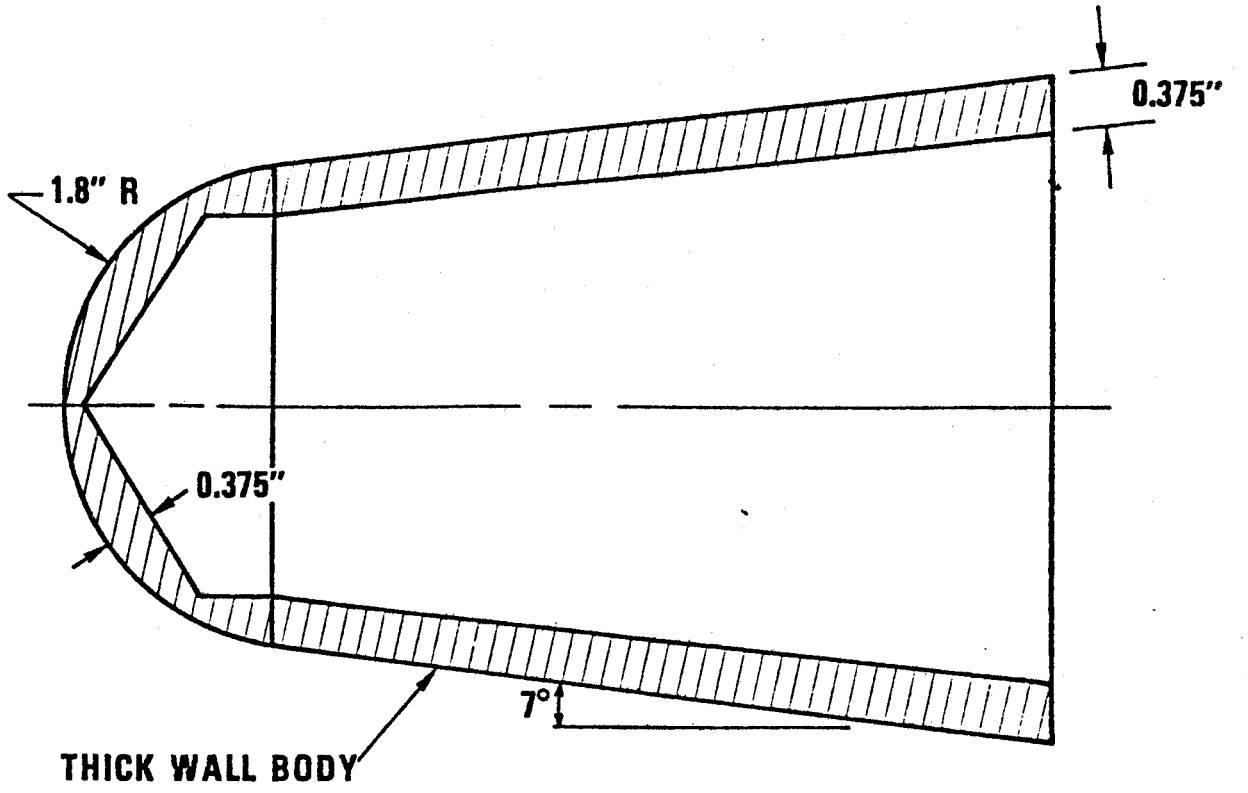

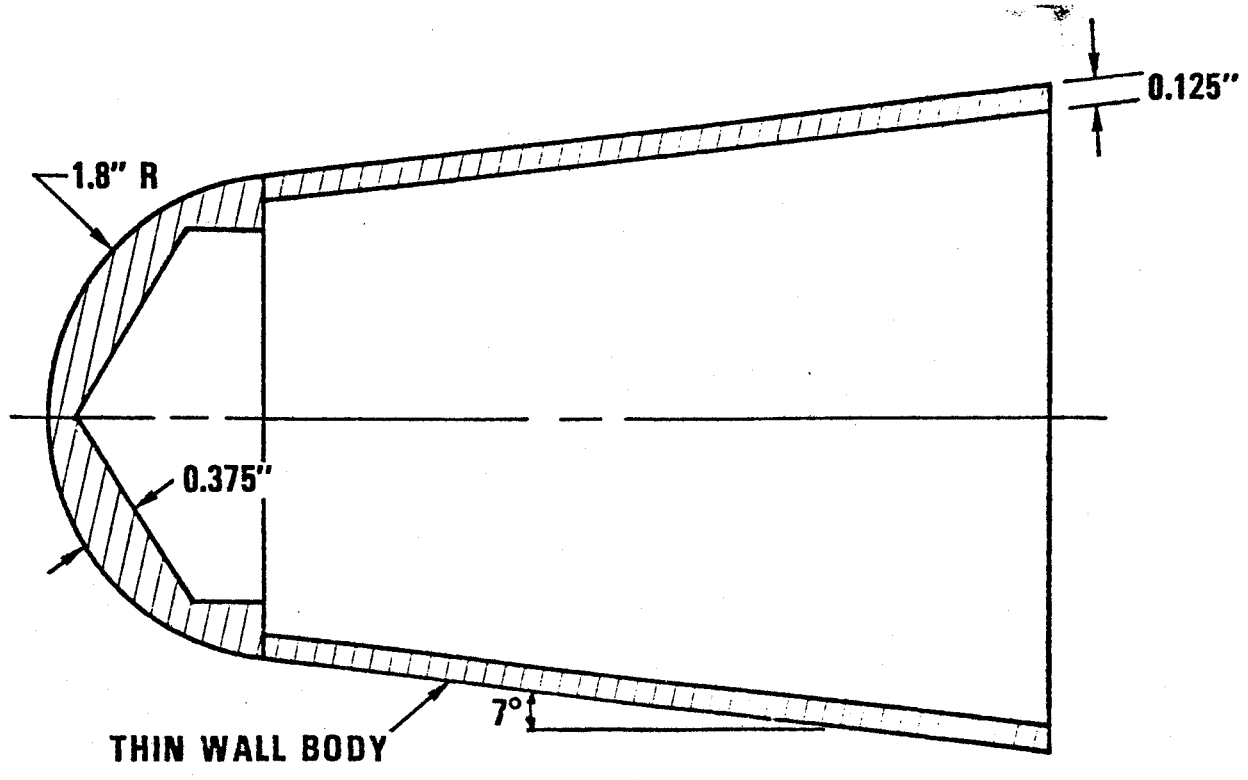

FIGURE 4 - MODEL CONFIGURATIONS FOR SHAKEDOWN TEST

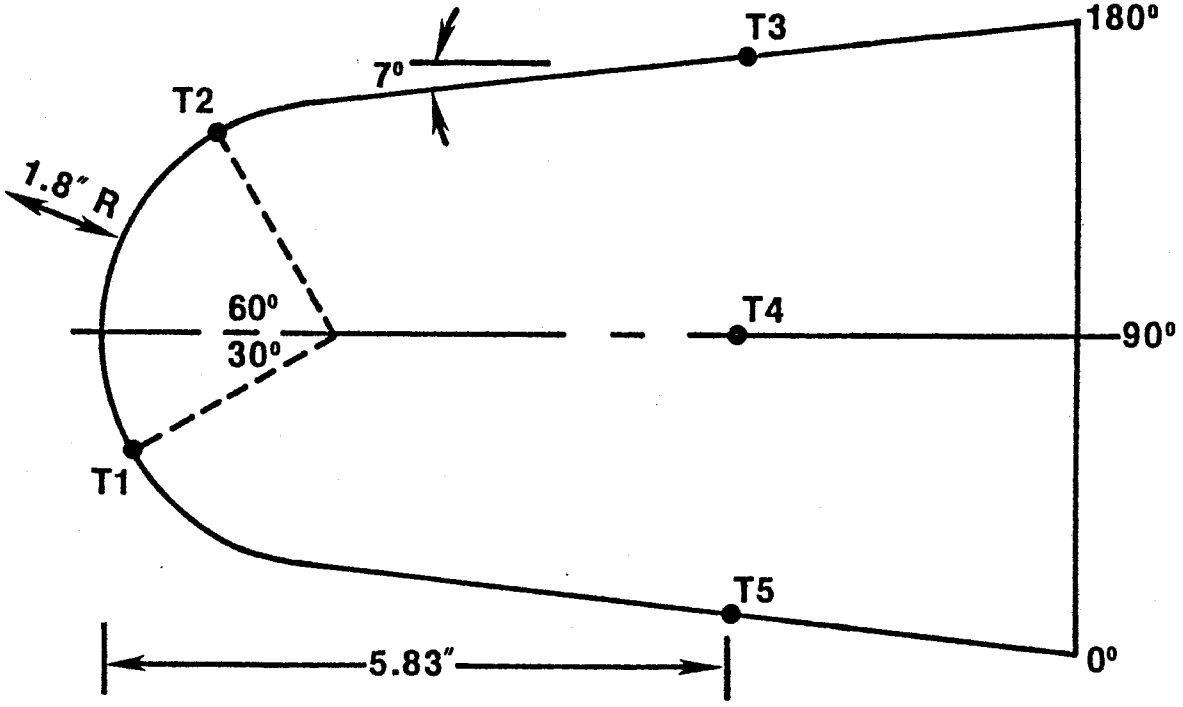

MODEL MATERIAL: 17-4 PH STAINLESS STEEL

FIGURE 5 - LOCATIONS OF COAXIAL THERMOCOUPLES FOR SHAKEDOWN TEST

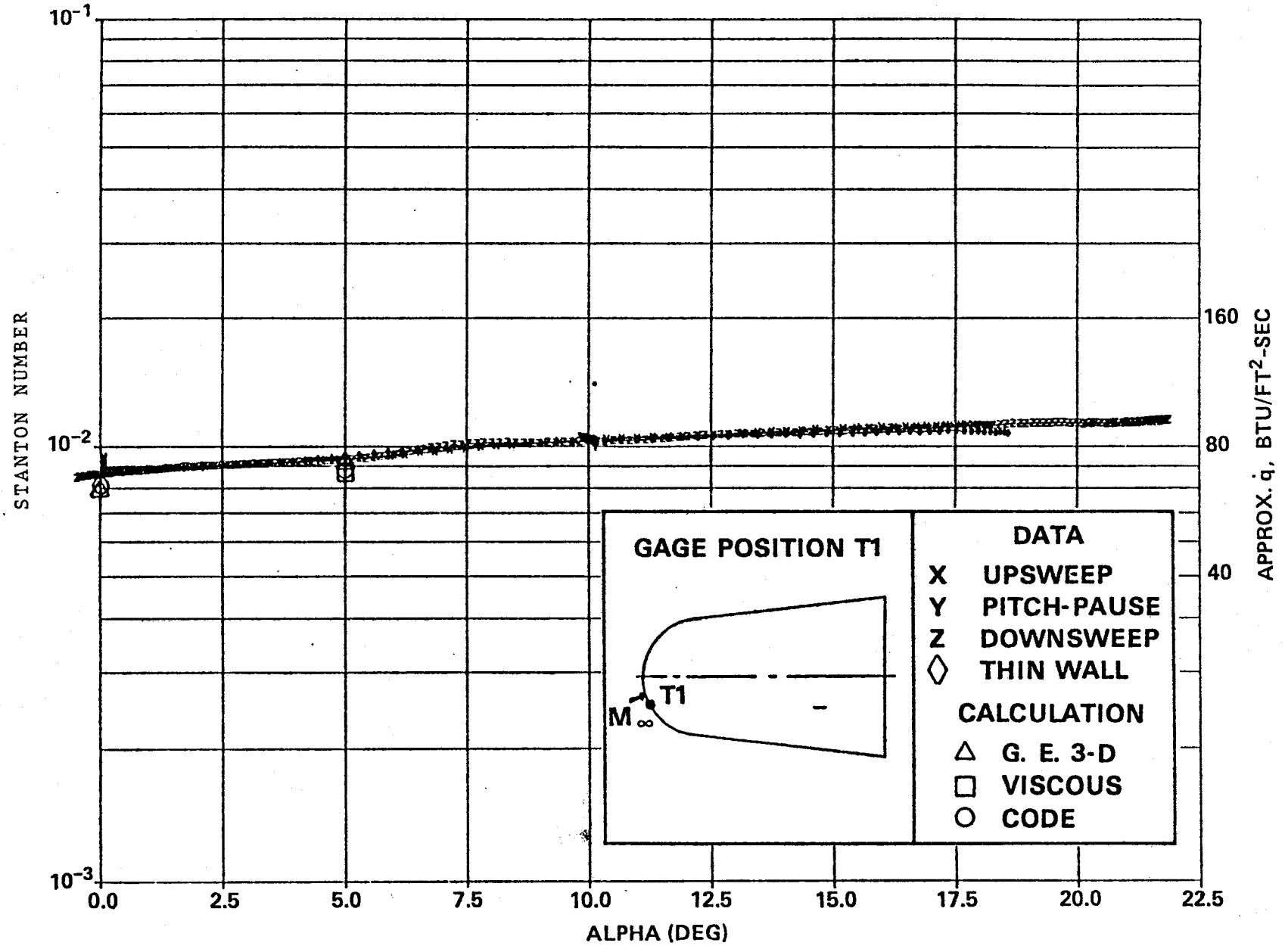

FIGURE 6 - STANTON NUMBERS FOR THERMOCOUPLE NO. 1

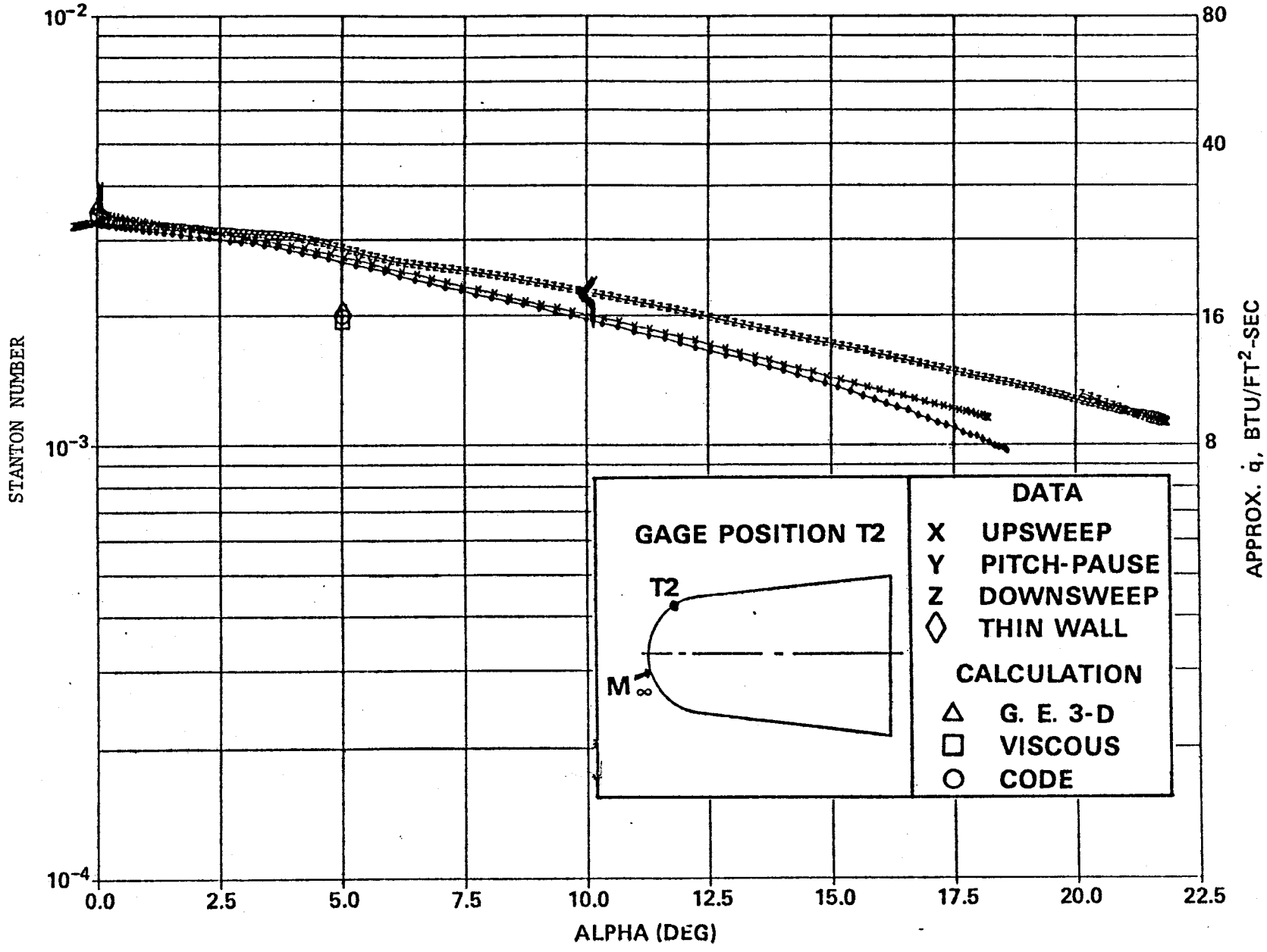

FIGURE 7 - STANTON NUMBERS FOR THERMOCOUPLE NO. 2

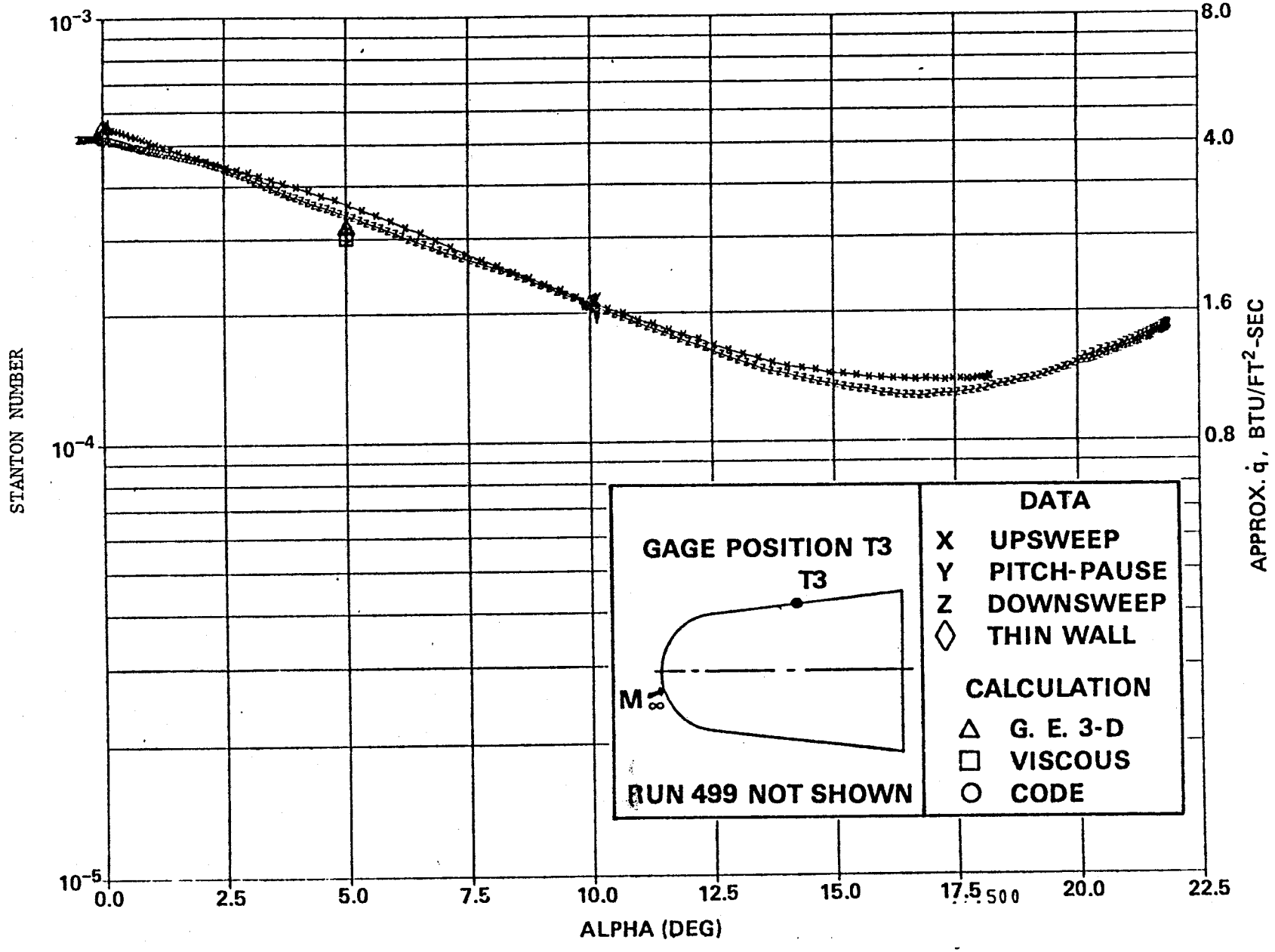

FIGURE 8 - STANTON NUMBERS FOR THERMOCOUPLE NO. 3

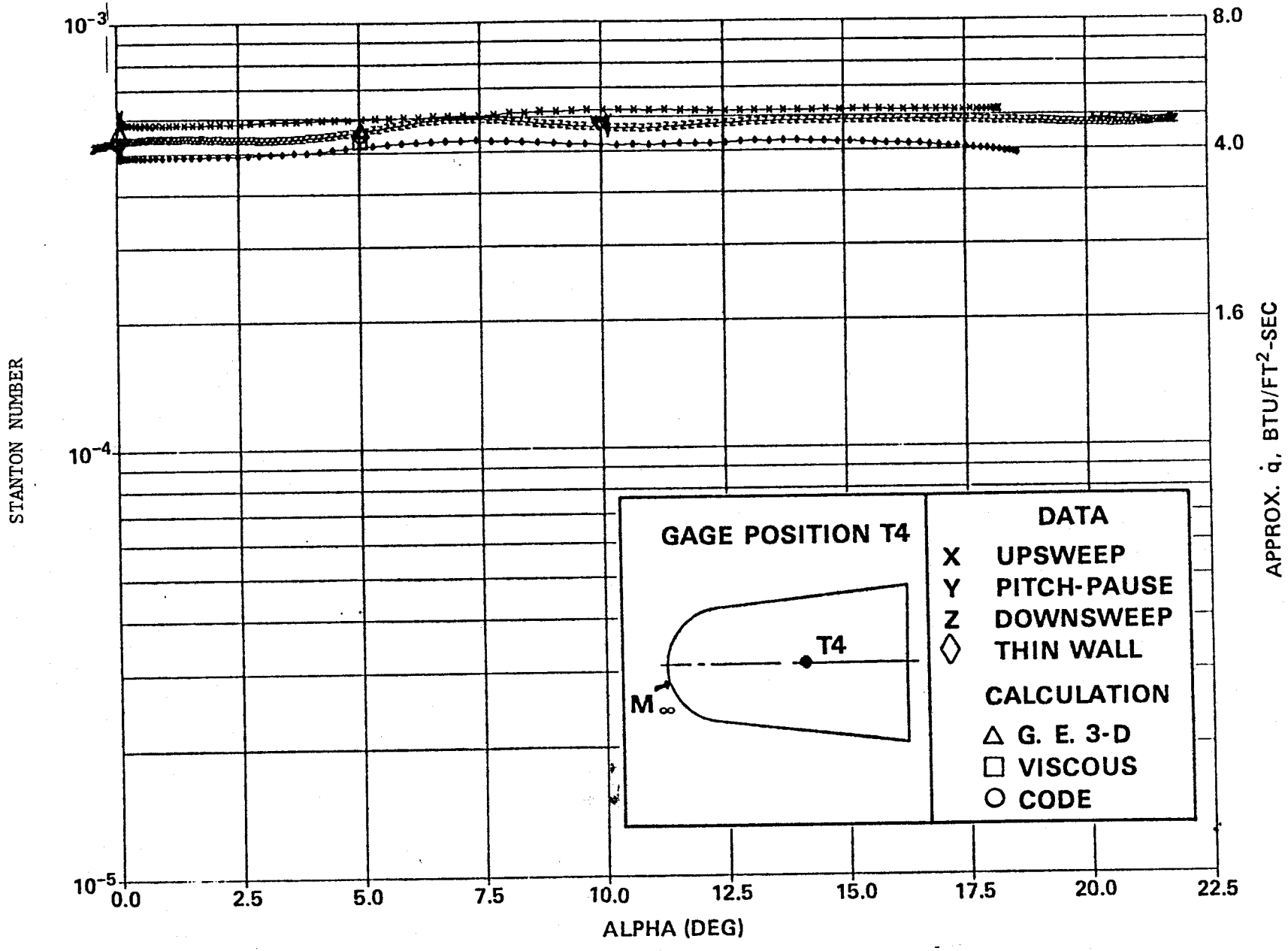

FIGURE 9 - STANTON NUMBERS FOR THERMOCOUPLE NO. 4

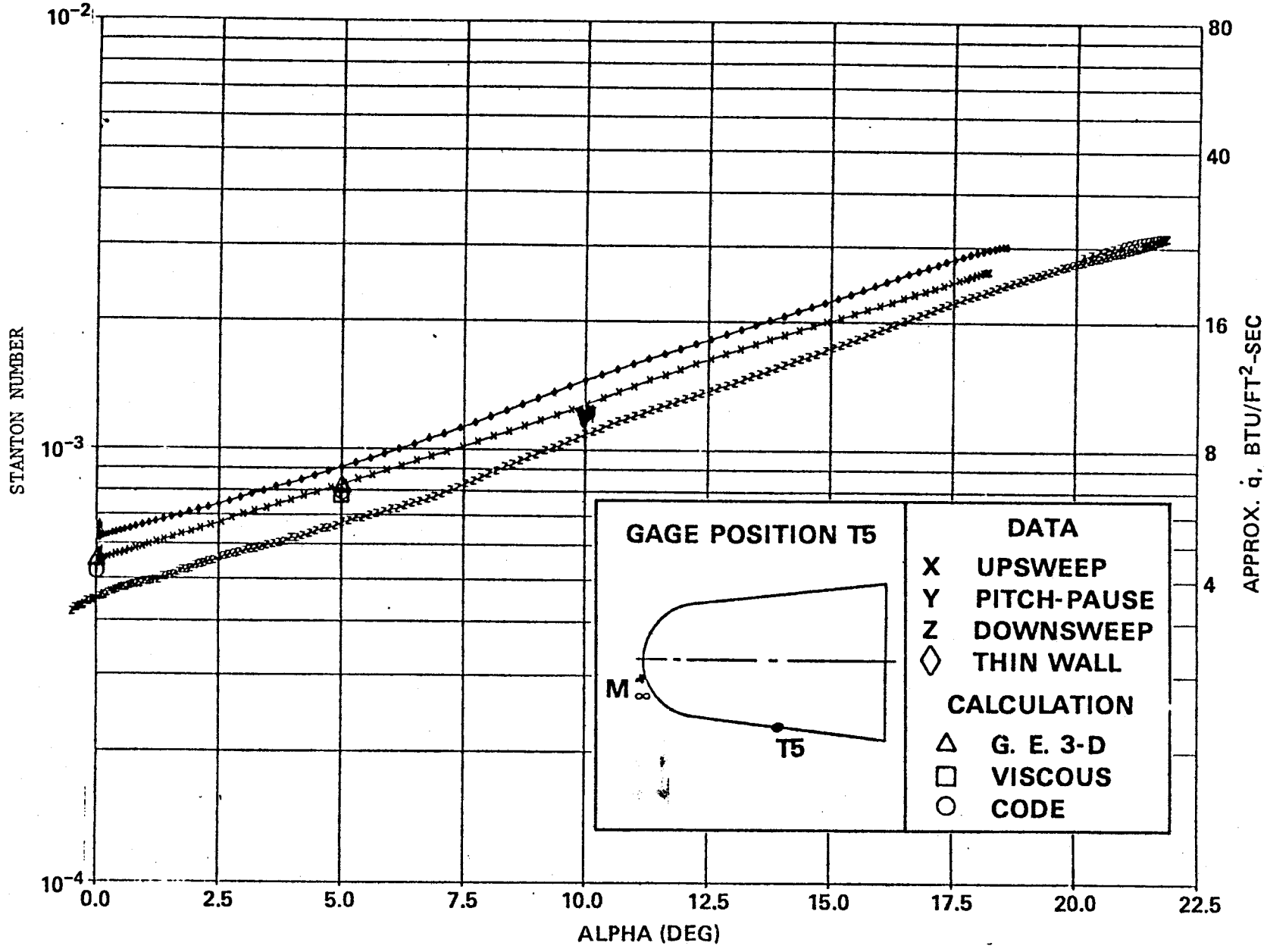

FIGURE 10 - STANTON NUMBERS FOR THERMOCOUPLE NO. 5

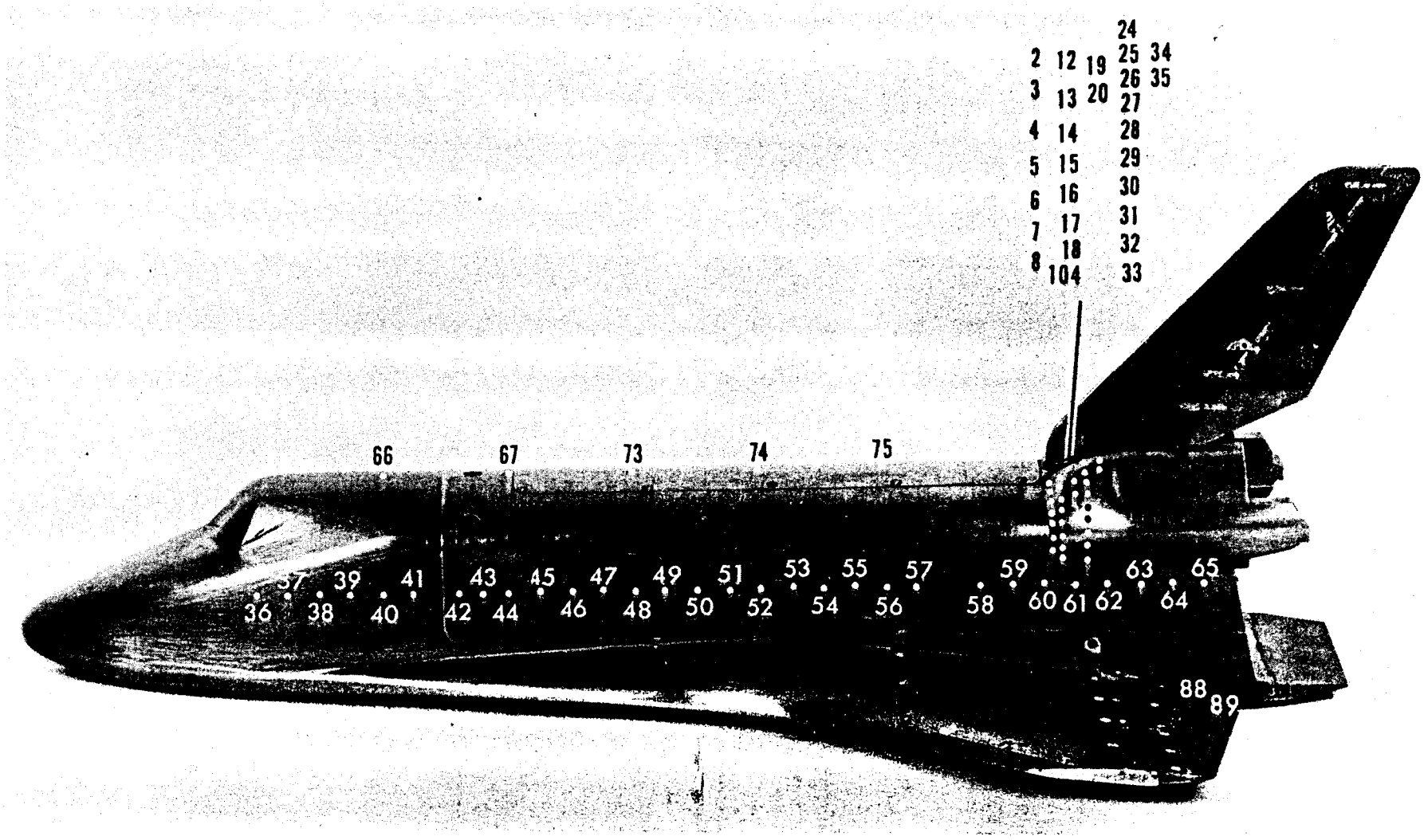

FIGURE 11 COAXIAL THERMOCOUPLE GAGE LOCATIONS IN 1.75 PERCENT SCALE SPACE SHUTTLE MODEL